1. INTRODUCTION

Earthquake ground motion time histories at different locations on the ground surface of an engineering site inevitably vary owing to wave propagation effects. Spatially varying ground motion affects structural responses, especially large space structures. It might excite some of structural vibration modes that would not be excited by uniform ground motions, such as torsional modes of symmetric structures. It might also cause relative responses between adjacent structures that lead to pounding or unseating of bridge decks. In some cases, ground motion spatial variation effect might govern the structural response and consequently determine the structural damage. To predict structural responses more realistically it is therefore important to accurately model ground motion spatial variations.

There are few ground motion spatial variation models available in the literature [e.g. Sobczyk 1991, Bolt et al 1982, Abrahamson 1985, Harichandran and Vanmarke 1984, Hao 1989]. Except for the theoretical model derived by Sobczyk [1991], which was based on analysis of stochastic wave propagation in a homogeneous random field, all the other models were derived from recorded strong ground motions in dense arrays, such as the SMART-1 array in Taiwan. All the other models are one-dimensional with the loss of coherency depending on the separation distance, with the exception of the model derived by Hao [1989], which is a two dimensional model, i.e. the coherency loss between ground motions at various points on the ground surface depends on not only the separation distance, but also on the wave propagation direction. Because of the constraint of the array configuration, both the theoretical and empirical ground motion spatial variation relations are valid only to sites with flat surface and similar geological conditions. In reality, supports of extended structures could rest on sites of different conditions. One bridge pier could be on rock outcrop while another on soft soil. There is no spatial variation model in the literature to represent such ground motions.

This study presents results of theoretical derivations of ground motion spatial variation on a site with uneven surface and different site conditions, in particular, soil and rock. Wave propagation theory is used in the derivation. Site amplification and attenuation owing to damping of the site is considered. The ground motions at bedrock are assumed to have the same intensity but vary spatially. Spectrums and loss of coherency of motions on ground surface are derived. It should be noted that in the derivation the site is assumed to be homogeneous and no loss of coherency is induced due to wave propagation through the site.

2. THEORETICAL DERIVATIONS

Figure 1 illustrates the schematic view of the site under consideration, in which ρ and v represent density and shear wave velocity of the site material, and ξ is the damping ratio. Assume the seismic wave propagates into the site with an incident angle α, and then propagates vertically to ground surface. If the horizontal separation distance between points A' and B' at base rock, or A and B on ground surface is d, the time lag between the waves at A' and B' is then $\tau_R = d\cos\alpha / v_R$, in which v_R is the shear wave velocity of the base rock.

Let ground motion at A' and B', $u_A'(t)$ and $u_B'(t)$ have the same intensity, i.e. their power spectral density function $Su_A'(\omega) = Su_B'(\omega) = S_R(\omega)$. This assumption is valid because the separation distance d is much smaller than the epicentral distance. However, they are not perfectly cross-correlated owing to source mechanism and wave propagation effect in inhomogeneous path. The loss of correlation is represented by the theoretical loss of coherency function [Sobczyk 1991]

$$\gamma_{A'B'}(i\omega) = e^{-\beta\omega d^2 / v_R} \cdot e^{-i\omega d\cos\alpha / v_R} = \left|\gamma_{A'B'}\right| e^{-i\omega d\cos\alpha / v_R} \qquad (1)$$

where ω is circular frequency and β is a coefficient depending on the level of coherency loss. The cross power spectral density function between $u_A'(t)$ and $u_B'(t)$ then can be expressed as

$$S_{u_{A'}u_{B'}}(i\omega) = S_R(\omega)\gamma_{A'B'}(i\omega) \qquad (2)$$

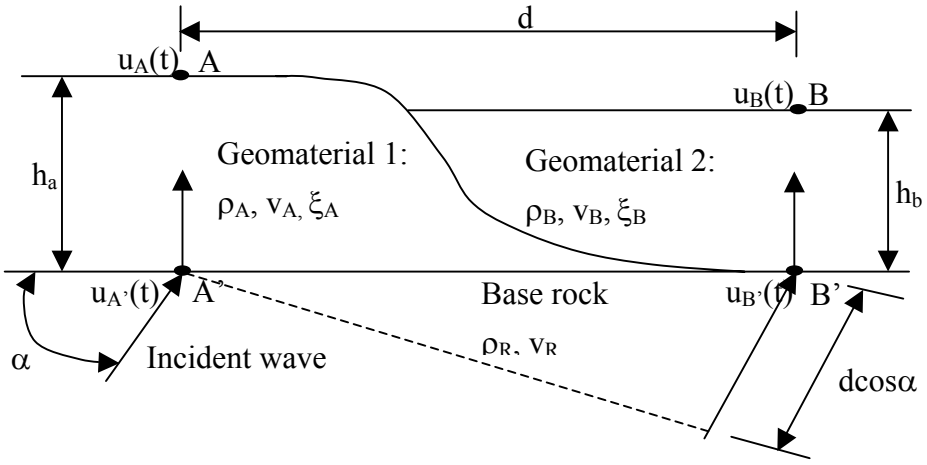

Figure 1 Schematic view of the site under consideration

Using wave propagation theory presented in [Aki and Richards 1980], Safak [1995] derived the transfer function for a shear wave propagating in a horizontal layer as

$$\frac{U_j(i\omega)}{U_{j'}(i\omega)} = \frac{2(1+r_j - i\xi_j)e^{-i\omega\tau_j(1-2i\xi_j)}}{1+(r_j - i\xi_j)e^{-2i\omega\tau_j(1-2i\xi_j)}} = H_j(i\omega) \tag{3}$$

where *'j'* represents A or B in this paper, $U_j(i\omega)$ is the Fourier transform of the $u_j(t)$, ξ_j is the damping ratio accounting for energy dissipation owing to wave propagation, and $\xi_j=1/4Q$, in which Q is the quality factor [Knopoff 1964]; $\tau_j=h_j/v_j$ is the wave propagation time from point *j'* at base rock to point *j* on ground surface, and r_j is the reflection coefficient for upgoing waves,

$$r_j = \frac{\rho_R v_R - \rho_j v_j}{\rho_R v_R + \rho_j v_j} \tag{4}$$

In engineering application, usually the outcrop motion on rock surface is available, instead of the base rock motion. If the outcrop motion is used, the constant 2 in Equation (3), which is a measure of free surface reflection, in the transfer function can be dropped. Then it has

$$\frac{U_j(i\omega)}{U_{j'}(i\omega)} = \frac{(1+r_j - i\xi_j)e^{-i\omega\tau_j(1-2i\xi_j)}}{1+(r_j - i\xi_j)e^{-2i\omega\tau_j(1-2i\xi_j)}} = H_j(i\omega) \qquad j = A \text{ or } B \tag{5}$$

The motion on ground surface is therefore

$$U_A(i\omega) = H_A(i\omega)U_{A'}(i\omega) \tag{6}$$

and similarly

$$U_B(i\omega) = H_B(i\omega)U_{B'}(i\omega) \tag{7}$$

The power spectral density functions of the motion on ground surface are

$$S_{uA}(\omega) = \frac{1}{2\pi T} H_A(i\omega)U_{A'}(i\omega)U^*_{A'}(i\omega)H^*_A(i\omega) = \left|H_A(i\omega)\right|^2 S_R(\omega) \tag{8}$$

and

$$S_{uB}(\omega) = \frac{1}{2\pi T} H_B(i\omega)U_{B'}(i\omega)U^*_{B'}(i\omega)H^*_B(i\omega) = \left|H_B(i\omega)\right|^2 S_R(\omega) \tag{9}$$

in which T is the duration of the ground motion and superscript '*' represents complex conjugate. The cross power spectral density function of ground motion at A and B is

$$\begin{aligned} S_{uAuB}(i\omega) &= \frac{1}{2\pi T} H_A(i\omega)U_{A'}(i\omega)U^*_{B'}(i\omega)H^*_{B'}(i\omega) = H_A(i\omega)H^*_B(i\omega)S_{uA'uB'}(i\omega) \\ &= H_A(i\omega)H^*_B(i\omega)\gamma_{A'B'}(i\omega)S_R(\omega) \end{aligned} \tag{10}$$

The coherency loss between ground motions at points A and B is

$$\begin{aligned} \gamma_{AB}(i\omega) &= \frac{S_{uAuB}(i\omega)}{\sqrt{S_{uA}(\omega)S_{uB}(\omega)}} = \frac{H_A(i\omega)H^*_B(i\omega)\gamma_{A'B'}(i\omega)}{\sqrt{\left|H_A(i\omega)\right|^2\left|H_B(i\omega)\right|^2}} \\ &= e^{-i[\theta_A(\omega)-\theta_B(\omega)]}\gamma_{A'B'}(i\omega) \\ &= \left|\gamma_{A'B'}(i\omega)\right| e^{-i[\theta_A(\omega)-\theta_B(\omega)+\omega d\cos\alpha/v_R]} \end{aligned} \tag{11}$$

where $\theta_A(\omega)$ and $\theta_B(\omega)$ are the phase angles of the transfer function $H_A(i\omega)$ and $H_B(i\omega)$, respectively.

2.1 Special Case 1: $h_b=0.0$ m

In that case, $r_B=1.0$, $\xi_B=0.0$ and $\tau_B=0.0$. Substitute these into the transfer function (5), it has $H_B(i\omega)=1.0$, or $U_B(i\omega)=U_{B'}(i\omega)$. Then $S_{uB}(\omega)=S_R(\omega)$, $\theta_B(\omega)=0$ and $\gamma_{AB}(i\omega) = e^{-i\theta_A(\omega)}\gamma_{A'B'}(i\omega)$.

2.2 Special Case 2: $h_a=h_b$, $v_A=v_B$, $\rho_A=\rho_B$

This case corresponds to a uniform horizontal layer above the base rock. From Equations (4) and (5), it can be derived that $S_{uA}(\omega) = S_{uB}(\omega) = |H_A(i\omega)|^2 S_R(\omega)$, $\theta_A(\omega)=\theta_B(\omega)$, and $\gamma_{AB}(i\omega) = \gamma_{A'B'}(i\omega)$.

2.3 Special Case 3: $h_a=h_b$, $v_A\neq v_B$, and $\rho_A\neq\rho_B$

In this case, points A and B have the same elevation, but are on sites of different properties. The above derived equations (8) to (11) for power spectral density function and coherency loss function for motions at A and B should be used.

The power spectral density function of the motion at the base rock, $S_R(\omega)$, can be determined either from the given response spectrum of the site, or from the attenuation function such as those developed for east Northern America [Atikson and Boore 1995], or that for southwest Western Australia [Hao and Gaull 2004]. In this study, however, the very popularly used filtered Tajimi-Kanai function is applied [Ruiz and Penzien 1969],

$$S_R(\omega) = \frac{\omega_g^4 + (2\xi_g\omega_g\omega)^2}{(\omega_g^2-\omega^2)^2 + (2\xi_g\omega_g\omega)^2} \frac{\omega^4}{(\omega_1^2-\omega^2)^2 + (2\xi_1\omega_1\omega)^2} S_0 \qquad (12)$$

where $\omega_1=1.636$, $\xi_1=0.619$ are the central frequency and damping ratio of the high pass filter, and ω_g and ξ_g are the central frequency and damping ratio of the Tajimi-Kanai spectrum. They are assumed to be 31.4 rad/s and 0.6 respectively in this study.

3. NUMERICAL CALCULATIONS

Using the theoretical power spectral density function and coherency loss function derived above, ground motion intensity and spatial variation can be estimated.

Figure 2 shows the base rock motion power spectral density function and coherency loss function used in this study. The parameter S_0 (Equation (12)) depends on the ground motion amplitude and duration. In the present study, $S_0=1.0$ is assumed. The coherency loss function is estimated with the assumption that the separation distance

$d=50$ m, and the coefficient $\beta=0.01,0.02$, and 0.05 for highly, intermediately and weakly correlated motions, respectively. The base rock has the shear wave velocity $v_R=3900$ m/s and density $\rho_R=2700\ kg/m^3$. The wave incident angle α is 60°.

To investigate the effect of the stiffness of the layers A and B on site amplification the amplitude of the site transfer function, surface motion power spectral density function, and phase angle of the transfer function are calculated with the assumption that $\rho_A=2500\ kg/m^3$, $\rho_B=2000\ kg/m^3$, and $h_a=h_b=30\ m$. Figure 3 shows the amplitude of the transfer function with varying shear wave velocity of the site. The peak of the transfer function occurs at the fundamental vibration frequency of the site, $f_i=v_i/4h_i$, where $i=A$ or B.

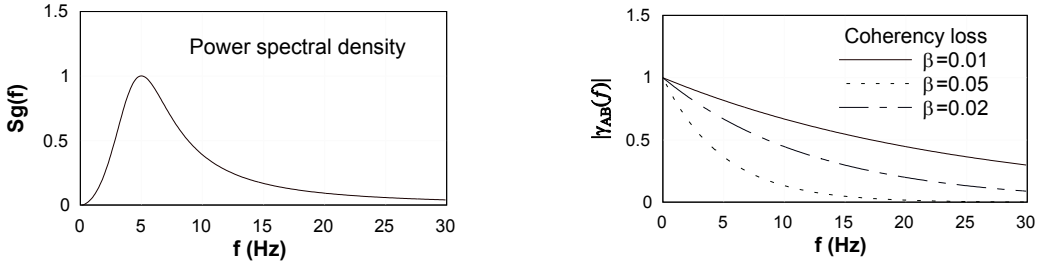

Figure 2. Base rock motion power spectral density function and coherency loss function (β=0.01, highly, β=0.02, intermediately and β=0.05, weakly correlated)

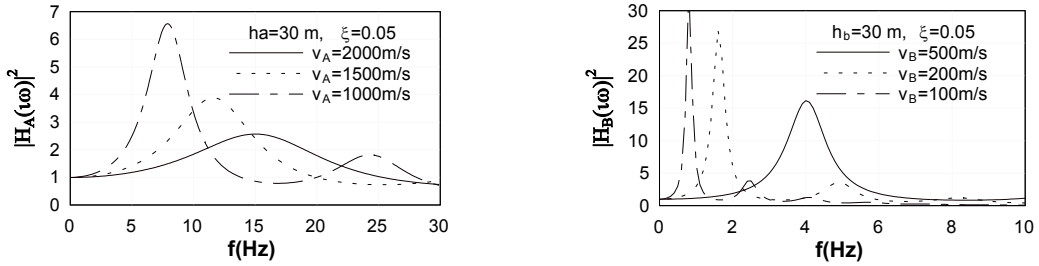

Figure 3 Transfer functions of the layer A and B

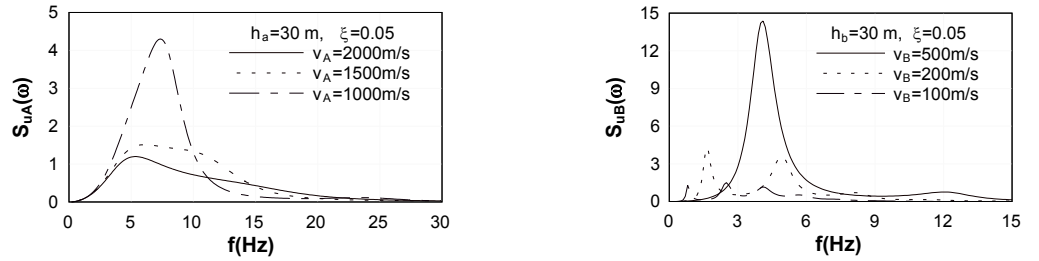

Figure 4 Power spectral density function of the surface motion

Figure 4 shows the corresponding power spectral density function of the surface ground motion. As shown, both layers A and B in general amplify the base rock motion. The amplification is most significant when the layer resonates with the incoming base rock motion. As shown, although the transfer function value for $v_B=100\ m/s$ and 200

m/s are similar and they are much larger than the one for v_B*=500 m/s*, the surface motion for v_B*=100 m/s* is very small, indicating the soft layer deamplifies the base rock motion. Figure 5 shows the phase angle of the transfer function for the two layers. These phase angles affect the phase differences of the surface motion. The phase angles vary between -π/2 and π/2, and are dependent on the shear wave velocity of the layer.

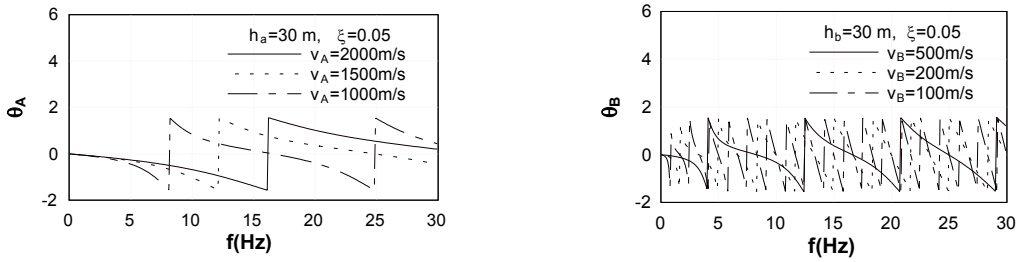

Figure 5 Phase angles of the transfer functions for the two layers

To investigate the effect of layer depth, the transfer function of the two layers, power spectral density function of the surface motion and phase angle of the transfer function are calculated. The shear wave velocities of the two layers are assumed to be v_A*=1500 m/s* and v_B*=200 m/s,* respectively. The numerical results are shown in Figures 6 to 8. As shown, when h_b*=0 m*, the transfer function is 1.0. Similar observations were made in Figures 2, 3 and 4. Soft layer always amplifies the base rock motion, and the amplification is most significant when the layer resonates with the incoming motion.

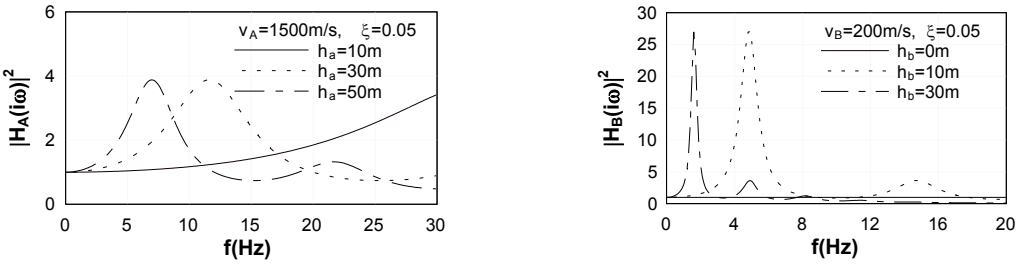

Figure 6 Transfer function of the two layers with different layer depth

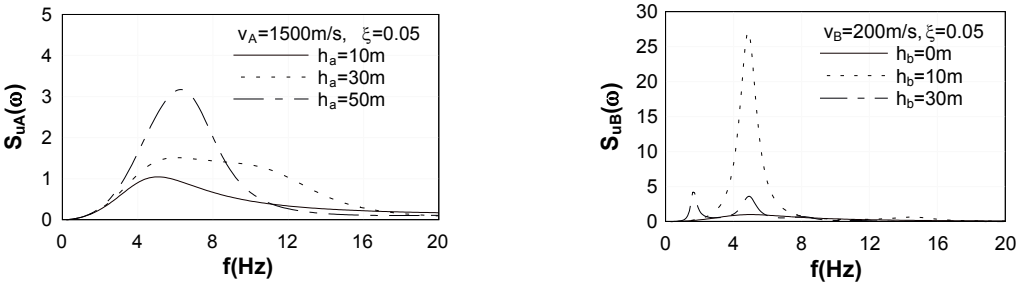

Figure 7 Surface motion power spectral density functions for different layer depths

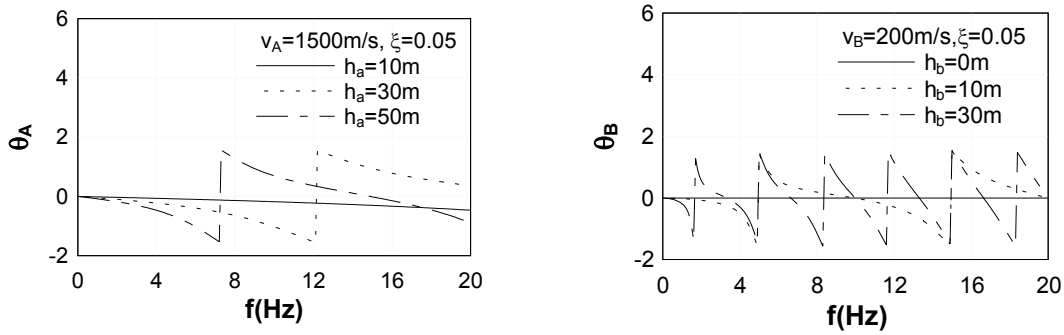

Figure 8 Phase angles of the transfer functions for different layer depth

4. CONCLUSIONS

Theoretical derivation of seismic motion spatial variation was carried out with consideration of local site amplification effect. The soil layer usually amplifies the base rock motion and changes the phase difference between base rock motions at any two points. The derived surface motion power spectral density function and spatial variation function can be used as the multiple inputs in dynamic structural response analysis.

REFERENCES

Abrahamson, NA. (1985) Estimation of seismic wave coherency and rupture velocity using the SMART-1 Strong Motion Array Recordings, Report No UCB/EERC-85-2, Earthquake Eng Res Center, University of California at Berkeley.

Aki, K and Richards, PG. (1980) Quantitative seismology theory and methods, W.H. Freman and Co., San Francisco, California.

Atkinson GM and Boore DM. (1995) New ground motion relations for eastern North America, Bull. Seism. Soc. Am., Vol. 85, pp17-30.

Bolt, BA, Loh, CH, Penzien, J, Tsai, YB and Yeh, YT. (1982), Preliminary report on the SMART-1 Strong Motion Array in Taiwan, Report No. UCB/EERC-82-13, Earthquake Eng Res Center, University of California at Berkeley.

Hao, H (1989), Effects of spatial variation of ground motions on large multiply-supported structures, Report No. UCB/EERC-89-06, Earthquake Eng Res Center, University of California at Berkeley.

Hao, H. and Gaull, BA. (2004) Prediction of Seismic Ground Motion in Perth Western Australia for Engineering Application, Paper No. 1892, Proceedings of the 13Th World Conference on Earthquake Engineering, August 2004, Vancouver, Canada.

Harichandran, R and Vanmarcke, E (1984). Space-time variation of earthquake ground motion, Research report R84-12, Dept. of Civil Eng., MIT.

Knopoff, L. (1964). "Q" , Geophysics Review, Vol. 2, pp625-660.

Ruiz, P. and Penzien, J. (1969). Artificial generation of earthquake accelerograms, Report No. UCB/EERC-69-03, Earthquake Eng Res Center, University of California at Berkeley.

Safak, E. (1995). Discrete-time analysis of seismic site amplification, Journal of Engineering Mechanics, ASCE, Vol. 121(7), pp801-809.

Sobczyk, K. (1991). Stochastic wave propagation, Kluwer Academic Publishers, the Netherlands.